

C(sp³)-F Bond Activation by Lewis Base-Boryl Radicals via Concerted Electron-Fluoride Transfer

Xueying Guo,¹ Yuchen Zhang,¹ Xiaoyu Lai,¹ Yubing Pang,³ Xiao-Song Xue^{1,2*}

¹ Key Laboratory of Fluorine and Nitrogen Chemistry and Advanced Materials and Shanghai-Hong Kong Joint Laboratory in Chemical Synthesis, Shanghai Institute of Organic Chemistry, Chinese Academy of Sciences, Shanghai 20032, China

² School of Chemistry and Materials Science, Hangzhou Institute of Advanced Study, University of Chinese Academy of Science, Hangzhou 310024, China

³ Shanghai Key Laboratory for Molecular Engineering of Chiral Drugs, Center for Ultrafast Science and Technology, Frontiers Science Center for Transformative Molecules, School of Chemistry and Chemical Engineering, Shanghai Jiao Tong University, Shanghai 200240, China

Abstract

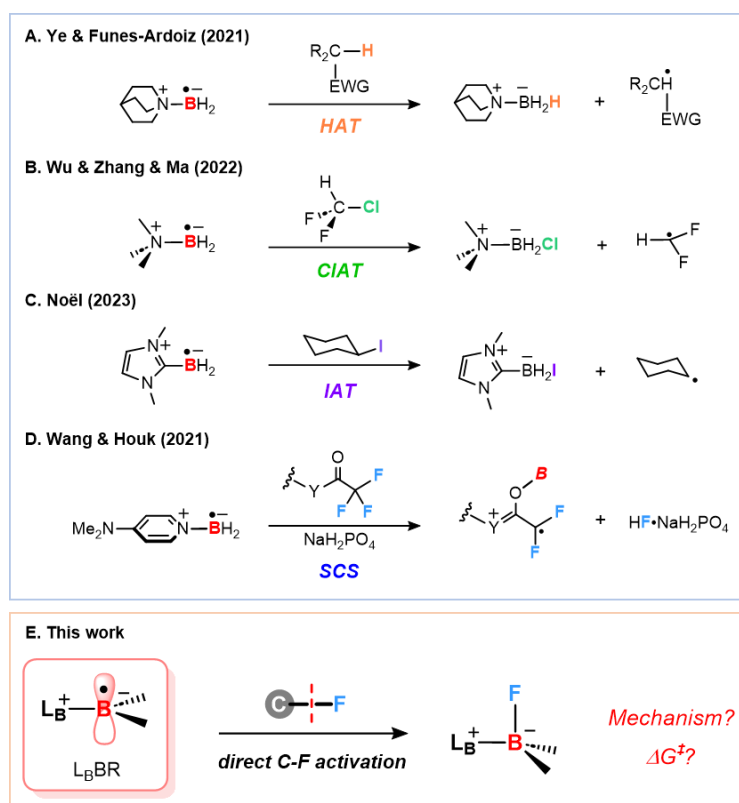
Selective C–F bond activation through a radical pathway in the presence of multiple C–H bonds remains a formidable challenge, owing to the extraordinarily strong bond strength of the C–F bond. By the aid of density functional theory calculations, we disclose an innovative concerted electron-fluoride transfer mechanism, harnessing the unique reactivity of Lewis base-boryl radicals to selectively activate the resilient C-F bonds in fluoroalkanes. This enables the direct abstraction of a fluorine atom and subsequent generation of an alkyl radical, thus expanding the boundaries of halogen atom transfer reactions and adding a new strategy to the C-F bond activation toolkit.

Introduction

Recent advancements in radical chemistry have witnessed the rise of Lewis base-boryl radicals (**L_BBRs**).^[1] These entities have been utilized in a multitude of chemical transformations,^[2] and their role as mediators for hydrogen atom transfer (**HAT**)/halogen atom transfer (**XAT**) has been especially noteworthy.^[3] For example, Ye, Funes-Ardoiz, *et al.* reported successful hydroalkylation of unactivated olefins by using an amine-boryl radical that selectively activates the electron-deficient C-H bond through **HAT** (**Scheme 1**).^[4] Moreover, Wu *et al.* have demonstrated the first example of introducing CF₂H moiety into alkenes from selective activation of ClCF₂H (Freon-22) through chlorine atom transfer (**CIAT**) mediated by another amine-ligated boryl radical.^[5] Very recently, Noël *et al.* showcased the utility of NHC-boryl radical to forge C(sp³)-C(sp³) bond formation via iodine atom transfer (**IAT**) processes, expanding the arsenal of radical-mediated transformations.^[6]

Despite these remarkable advances, selective C(sp³)-F bond activation through fluorine atom transfer remains a daunting challenge due to the high thermodynamic stability and kinetic inertness of these bonds.^[7] This challenge is intensified when multiple C–H bonds are present alongside the aliphatic C(sp³)-F bond.^[8] Only recently has Wang, Houk and coworkers reported the first C-F functionalizations of trifluoroacetic acid derivatives by **L_BBR** through a spin-center-shift (**SCS**) strategy.^[9] In this communication, we present our theoretical investigations of direct and selective C-F activation by **L_BBRs** via concerted electron-fluoride transfer (**cEF-T**) mechanism. This enables the

direct abstraction of a fluorine atom from fluorocarbons and the generation of an alkyl radical, thereby broadening the scope of **XAT** reactions. Traditionally, **XAT** reactions have been primarily limited to organic halides containing chlorine, bromine, and iodine.^[3c]

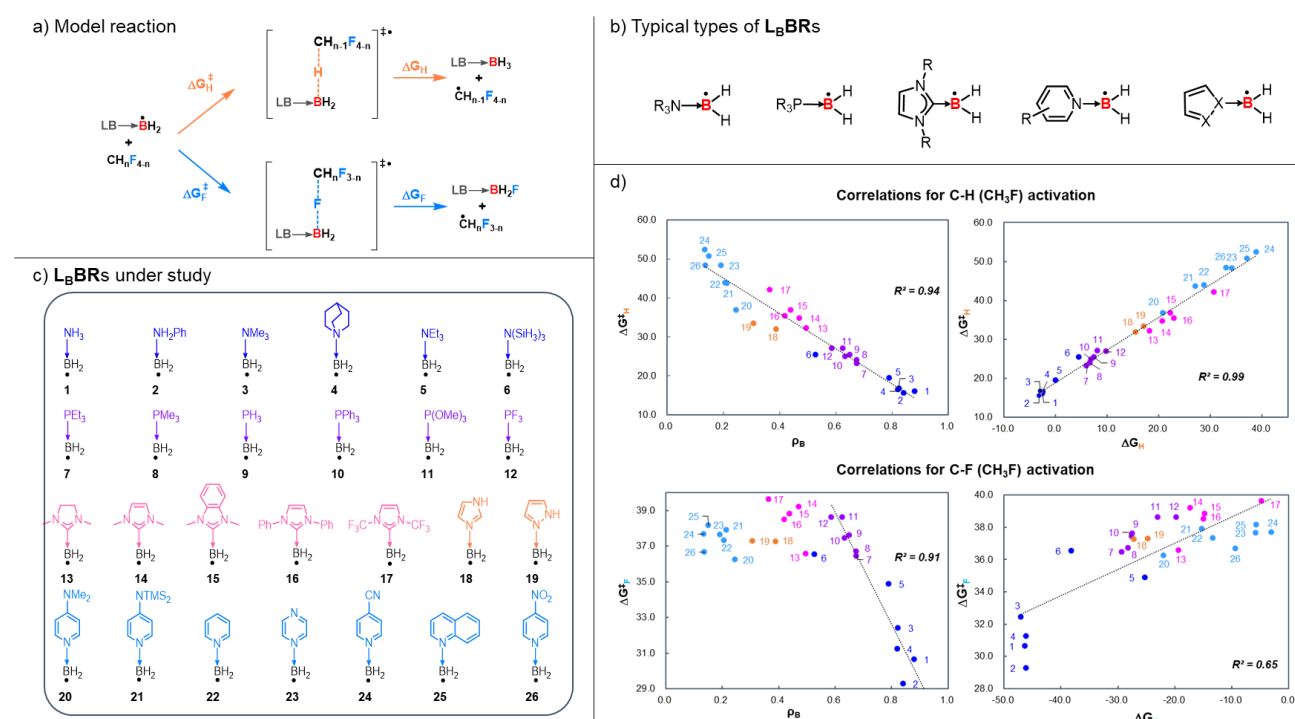


Scheme 1. Selected examples of **L_BBRs** mediated hydrogen atom transfer (**HAT**)/halogen atom transfer (**XAT**): (A) **HAT**, (B) **CIAT**, (C) **IAT**, (D) C-F functionalization through **SCS** mediated by **L_BBRs** reported by previous work, (E) Direct C-F activation by **L_BBRs** studied in this work.

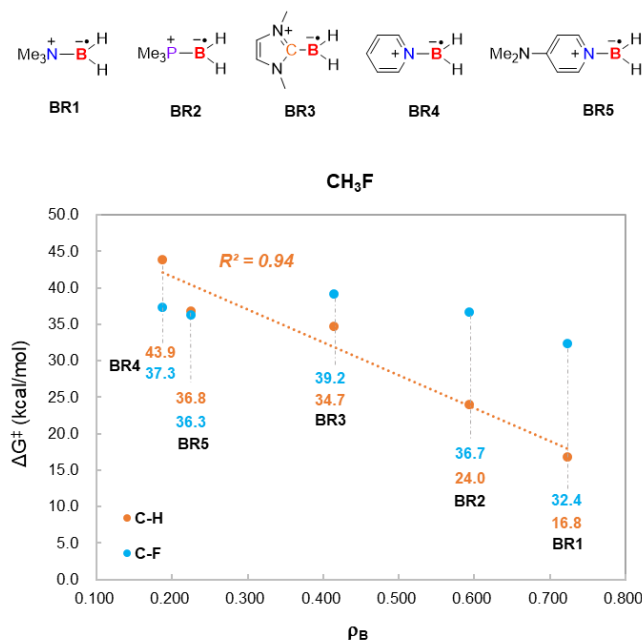
Results and Discussion

To facilitate the investigation, C-H/F activation of fluoroalkane ($\text{CH}_n\text{F}_{4-n}$) by **L_BBRs** is chosen as the model reaction (**Scheme 2a**). Initially, 26 **L_BBRs** with several typical kinds of **L_Bs**, including amines, phosphines and various heterocyclic ligands (NHCs, pyridines, etc.) were studied. To describe the reactivity of these **L_BBRs**, the Hirshfeld spin population of the boron center (denoted as ρ_{B}) was chosen as an index, which can be interpreted as the delocalization extent of the spin density on the boron. It was reported by Rablen,^[10] Li^[11] and Cao^[12] that the spin population of boron has good linear correlations with B-H BDE of a series **L_BBRs**. We thereby examined the relationship between ρ_{B} and the activation energies of C-H and C-F activation, which is denoted as $\Delta G^\ddagger(\text{H})$ and $\Delta G^\ddagger(\text{F})$, as depicted in **Scheme 2d**. Calculation results show that for C-H activation, $\Delta G^\ddagger(\text{H})$ s have good linear relationships with ρ_{B} , i.e., the larger the ρ_{B} is, the lower the $\Delta G^\ddagger(\text{H})$ is. While for C-F activation, a good correlation is only found when ρ_{B} is larger than around 0.6 (amines and phosphines coordinated **BRs**). However, no clear correlation between $\Delta G^\ddagger(\text{F})$ and ρ_{B} is observed when ρ_{B} is smaller than 0.6 (heterocycles coordinated **BRs**). Similar correlations were also found for C-H/F activation of activations of CH_2F_2 and CHF_3 (see **Figure S1**). Drawing on the recent work by Doyle, Wu, Zhang, and co-workers,^[13] we further investigated the correlations between energy barriers (ΔG^\ddagger) and reaction energies (ΔG_0) for both C-H/F activation reactions. As illustrated in **Scheme 2**, an excellent correlation is found for C-H activation, which is in good accordance with the Bell-Evans-Polanyi

principle^[14], while the correlation for C-F activation is much poorer. From the initial investigations, we realized that the C-F activation must have different mechanism from the C-H activation. In addition, for the C-F activation, different reaction modes exist between different types of L_BBRs .



Scheme 2. (a) The model reaction under study, (b) Typical types of L_BBRs , (c) 26 L_BBRs under study, (d) Correlations of energy barriers ΔG^\ddagger (kcal/mol) against reaction energies ΔG_0 (kcal/mol) and spin density population of boron (ρ_B , a.u.) calculated for the C-H and C-F activation of CH_3F .



Scheme 3. Correlations of spin density population of boron (ρ_B , a.u.) with ΔG^\ddagger_H (kcal/mol) and ΔG^\ddagger_F (kcal/mol) of CH_3F for **BR1**~**5**.

To focus on revealing the mechanism, we narrow down the scope of our study and select five typical L_BBRs which are denoted as **BR1**~**5** (i.e., **3**, **8**, **14**, **20**, **22**) to dig out the mechanism of C-F activation and the factors that influence

the selectivity (**Scheme 3**). Taking the reactions with CH₃F as example (for CH₂F₂ and CHF₃, see SI), it shows that $\Delta G^\ddagger(\text{H})$ s is almost always lower than $\Delta G^\ddagger(\text{F})$ s, excepting the C-F activation of CH₃F by (Pyridine)BH₂• (**BR4**) and (DMAP)BH₂• (**BR5**). It is also interesting to note that the activation energy difference of $\Delta G^\ddagger(\text{H})$ and $\Delta G^\ddagger(\text{F})$ becomes smaller with the trend: **BR1** > **BR2** > **BR3** > **BR4** \approx **BR5**. Taking a closer look at the calculated energy barriers for the **BR1-5**. $\Delta G^\ddagger(\text{F})$ for **BR1** is the lowest (32.4 kcal/mol) but the $\Delta G^\ddagger(\text{H})$ is even lower (16.8 kcal/mol), indicating that **BR1** is highly selective for C-H activation, which is similar with **BR2**. For **BR3**, $\Delta G^\ddagger(\text{F})$ and $\Delta G^\ddagger(\text{H})$ are both high-lying, but $\Delta G^\ddagger(\text{F})$ is only 4.5 kcal/mol higher. For **BR4**, the $\Delta G^\ddagger(\text{F})$ is even lower than $\Delta G^\ddagger(\text{H})$ (37.3 vs. 43.9 kcal/mol) and **BR5** also having $\Delta G^\ddagger(\text{F})$ slightly lower. These results hinted that, the more σ -donating the **L_B** is, the lower the overall activation barriers. While the more π -accepting the **L_B** is, the C-F activation is more preferred. This is supported by the principal interacting spin orbital (**PISO**) analysis (refer to the discussion below).

In order to differentiate the reaction modes of the C-H and C-F activation by L_BBRs, we first compared the transition state (**TS**) by taking the reaction of **BR3** (NHC-BH₂•) as an illustration. It is remarkable to find the geometric difference between these two, as shown in **Figure 1A**. For **TS-BR3-H-CH₂F**, H-atom basically travels along the straight line between carbon and boron center. In contrast to the TSs for HAT and XAT processes previously described,^[15] the fluorine atom transfer (**FAT**) transition state structure **TS-BR3-F-CH₃** features an obtuse angle of C-F-B with 128.9°. In addition, the former TS is close to the B-H bond-forming product (a late TS), while the TS for the latter is close to the reactant (an early TS), which should be mainly due to the relatively high C-F bond strength.

To get further insights into the activation mechanism, we conducted the intrinsic bond orbital (**IBO**) analysis developed by Knizia and Klein,^[16] which is a powerful tool allowing visualization of the evolution in electronic structure along the intrinsic reaction coordinates (**IRC**). Knizia and Klein also reported the utilization of **IBO** to figure out **PCET** and **HAT** mechanisms in a straightforward manner.^[17] Here, we also apply this powerful method to distinguish the ambiguous electron transfer processes between C-H and C-F activations. In the case of C-H bond activation by **BR3**, IBO analysis unveiled that the α -electron of the C-H σ -bond and the unpaired electron of the boryl radical both transformed into the newly formed B-H σ -bond, while the β -electron of the C-H σ -bond remained on the carbon atom of the substrate (**Figure 1B**). This scenario supports a classical hydrogen atom transfer (**HAT**) process for the C-H activation.

The **FAT** process, however, proceeds with a different scenario. As depicted in **Figure 1C**, along with the F traveling from the carbon to the boron center, both the α - and the β -electron of the C-F σ -bond transformed into the newly formed B-F σ -bond, suggesting a fluoride transfer. Meanwhile, the unpaired electron of the boryl radical is transferred directly from **BR3** to the carbon center of the substrate. It can be interpreted that, with the F atom of CH₃F approaching the boron center, the unpaired electron of **BR3** can jump to the C-F σ^* -orbital and promote the delivery of fluoride to the empty orbital of the boron center. Such a process suggests a concerted electron-fluoride transfer (**cEFT**) mechanism instead of fluorine atom transfer. It is worth mentioning that Ritter and co-workers have raised a concept naming fluoride-coupled electron transfer (**FCET**)^[18], which was mainly applied to electrophilic or nucleophilic aromatic C-H fluorination.

Upon deciphering the mechanism of C-F bond activation, the effect of the L_B ligand is then explored. We carried out principal interacting spin orbital (**PISO**) analysis developed by Lin *et al*^[19] which is excel at interpreting orbital interactions between two fragments for open-shell systems. We divided the TS structures into two fragments across the C-B bond. Different interacting modes between the NHC ligand and the rest parts are delineated for **TS-BR3-F-**

CH₃ and **TS-BR3-H-CH₂F**, as shown in **Figure 2** and **Figure S4**. In **TS-BR3-F-CH₃**, a remarkable π interaction between NHC and BH₂-F-CH₃ moiety is found for the 1st α -PISO pair. The 2nd α -PISO pair is resembled with the 1st β -PISO pair, showing the σ -interaction between two fragments. Such picture manifests that the π^* orbital of the NHC ligand may have a stabilizing effect for the fluoride transfer process. On the other hand, in **TS-BR3-H-CH₂F**, the primary interactions for α - and β -PISO are both the σ interaction with equivalent PBIs and large contributions (>34%), saying that the σ -interaction is dominant here. While the π interaction found for α - and β -electron are both secondary with only minor contributions.

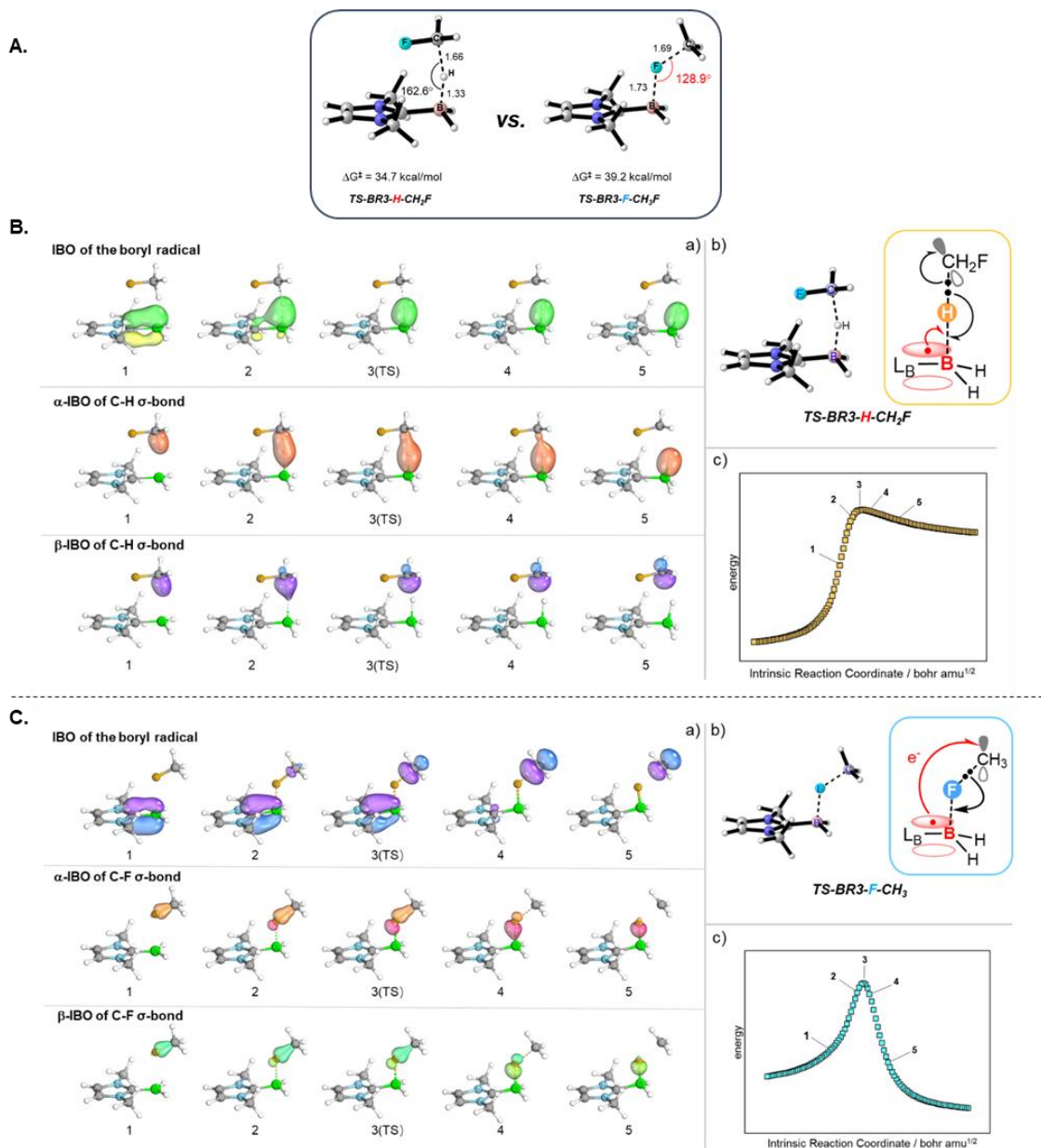


Figure 1. (A) Optimized structures of the TS for C-H and C-F activation of CH₃F by **BR3**, (B) IBOs calculated for the C-H bond activation and (C) IBOs calculated for the C-F bond activation of CH₃F by **BR3**. (a) The three key IBOs of the unpaired electron of the boryl radical, α -IBO, and β -IBO of the C-H/F σ -bond. (b) Schematic illustration of the HAT/cEF-T process. (c) IRC scheme for the transition state.

To further confirm whether the π -stabilization is important for fluoride transfer, PISO analysis was performed on the TS of the C-F activation by **BR1** which contains a σ -donating Me₃N ligand. As expected, the primary interaction

between the NMe_3 and the $\text{BH}_2\text{-F-CH}_3$ fragment is the σ -interaction for both α - and β -PISO, while a π -interaction is found in the second α -PISO pair which is very minor with a contribution of only 7.0% (**Figure S5**). This result is consistent with the fact that the **BR1** has the largest energy difference between $\Delta G^\ddagger(\text{H})$ and $\Delta G^\ddagger(\text{F})$ (refer to **Scheme 2**). It is also noticeable here that the TS shows an almost linear C-F-B geometry resembling an **FAT** process. While IBO analysis still manifests a **cEF-T** process (**Figure S6**), suggesting that different L_B ligands do not influence the reaction mechanism.

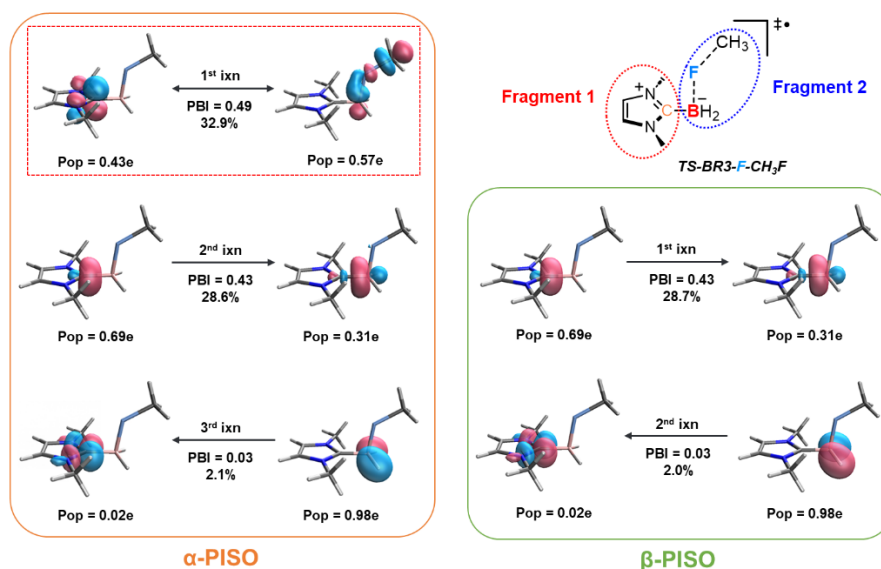
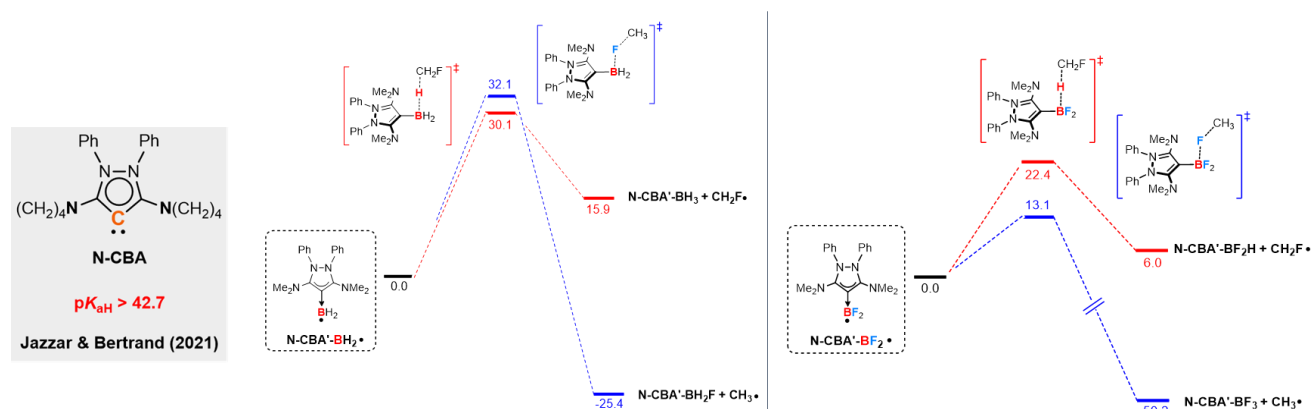


Figure 2. PISO pairs between the L_B fragment and the $\text{BH}_2\text{-F-CH}_3$ fragment for the transition state **TS-BR3-F-CH₃**. (Pop: PIO population of the indicated fragment; PBI: PIO-based bond index; %: percentage contribution of the PIO pair to the total orbital interactions.)

After learning the influence of the L_B ligands on the C-F bond activation, we next explored the role of various boryl substituents, as summarized in **Table S4**. Unexpectedly, when the boryl is substituted by $-\text{OH}$ and $-\text{F}$, the $\Delta G^\ddagger(\text{F})$ is lower than $\Delta G^\ddagger(\text{H})$. To understand the reason behind, PISO analysis was conducted on the $\text{NHC-BF}_2\bullet$ (**BR3-F**). A crucial interaction between the lone pairs of the two fluorine atoms and the π^* orbital of B-C bond/empty p orbital of boron is found (**Figure S7**), while such interaction is lacking in $\text{NHC-BH}_2\bullet$. We infer that such interaction elevates the energy of the π -bonding orbital between L_B and the boron center (SOMO), therefore facilitating the transferring of the unpaired electron to the C-F σ^* orbital for the **cEF-T** process, while suppressing the accepting of hydrogen atom for the HAT process. Indeed, checking the SOMO energies of these two, **BR3-F** is found to be higher than **BR3** (-4.99 vs. -5.36 eV). Besides, the strong electron-negative property of F could provide additional thermodynamic driving force to lower down the energy barrier.

At this stage, the nature of the mechanism and selectivity of the C-F activation by $\text{L}_\text{B}\text{BRs}$ is unraveled. To verify the operability of our understanding, we turn to seek an appropriate $\text{L}_\text{B}\text{BR}$ that can selectively activate C-F bond of fluoroalkane with an accessible activation energy. We consider a recently reported carbene species by Bertrand and co-workers, named **N-CBA**, which was found to be the most basic carbene.^[20] Such cyclic carbene ligand, containing a divalent C(0) center, is π -accepting as well as extremely σ -donating,^[21] which could have a strong tendency for C-F activation referring to our calculations. Here, we use the model **N-CBA'** with the amino group simplified to NMe_2 .

Our calculations for C-H and C-F activation of CH_3F by $\text{N-CBA}'\text{-BH}_2\bullet$ showed that $\Delta G^\ddagger(\text{H})$ is slightly lower than $\Delta G^\ddagger(\text{F})$ with energy barriers are 30.1 and 32.1 kcal/mol, respectively. (**Scheme 4**) When changing the boryl from BH_2 to BF_2 , we were excitingly to find that $\Delta G^\ddagger(\text{F})$ is much lower than $\Delta G^\ddagger(\text{H})$ with energy barriers of 13.1 and 22.4 kcal/mol, respectively. In addition, the C-F activation by $\text{N-CBA}'\text{-BF}_2\bullet$ is also found to be highly exothermic with a reaction energy of -50.2 kcal/mol. This implies that selective C-F bond activation through a radical pathway in the presence of multiple C-H bonds with $\text{N-CBA}'\text{-BF}_2\bullet$ is both kinetically and thermodynamically feasible. Until now, **XAT** reactions have commonly been confined to organic halides containing chlorine, bromine, and iodine. The direct abstraction of a fluorine atom from fluorocarbons along with the generation of an alkyl radical through a concerted electron-fluoride transfer mechanism, broadens the mechanism and scope of **XAT** reactions.^[3e] Referring to the synthesis of $\text{NHC-BF}_2\bullet$ reported by Curran, Lalevée and Lacôte,^[22] the synthesis of such $\text{N-CBA}'\text{-BF}_2\bullet$ may also be realized with a similar method. We look forward to the experimental validation of this prediction by synthetic chemists.



Scheme 4. Energy profiles for C-H and C-F activation by $\text{N-CBA}'\text{-BH}_2\bullet$ and $\text{N-CBA}'\text{-BF}_2\bullet$. The Gibbs free energies are given in kcal/mol.

Conclusion

In conclusion, our theoretical investigation has established a concerted electron-fluoride transfer mechanism that provides a radical strategic approach toward the selective activation of C-F bonds in fluoroalkanes. Rational design led us to conceive a Lewis base boryl radical that effectively combines π -accepting and strong σ -donating properties, together with the boryl substituents being strong σ withdrawing and π donating, thereby both kinetically and thermodynamically facilitating the cleavage of C-F bonds over C-H bonds. We anticipate that the insights obtained from our study will stimulate experimental chemists to explore suitable radical species that could selectively activate the inert C-F bond and develop sustainable methodologies for the transforming and repurposing of inert fluorocarbons.^[23] We foresee that this theoretical work will have far-reaching implications for **L_BBRs** design and applications in different contexts including radical chemistry, organic synthesis and catalysis.

ASSOCIATED CONTENT

Supporting Information

Computational details; Calculated Hirshfeld spin density population (B), activation energies (ΔG^\ddagger), and reaction energies (ΔG_0) for all **L_BBRs**; Supplementary correlations; Additional figures for IBO and PISO analysis; Calculated energy data and Cartesian coordinates for all the calculated species.

Notes

The authors declare no competing financial interest.

ACKNOWLEDGMENT

This work was supported by the Ministry of Science and Technology of China (2021YFF0701700), the National Natural Science Foundation of China (Nos. 22122104, 22193012, and 21933004), the CAS Project for Young Scientists in Basic Research (grant no. YSBR-095), the Shanghai Post-Doctoral Excellence Program (2022709), and the Strategic Priority Research Program of the Chinese Academy of Sciences (Grant No. XDB0590000). The numerical calculations in this study were carried out on the ORISE Supercomputer. The authors would also like to thank Professor Yi-Feng Wang from USTC and Dr. Fu Kit Sheong and Dr. Tilong Yang from HKUST for valuable discussions.

REFERENCES

- [1] For selected examples and reviews, see: (a) J. A. Baban, B. P. Roberts, *J. Chem. Soc., Chem. Commun.* **1983**, 1224-1226; (b) J. A. Baban, B. P. Roberts, *J. Chem. Soc., Perkin Trans. 2* **1988**, 1195-1200; (c) V. Paul, B. P. Roberts, *J. Chem. Soc., Perkin Trans. 2* **1988**, 1895-1901; (d) B. P. Roberts, *Chem. Soc. Rev.* **1999**, *28*, 25-35; (e) S.-H. Ueng, M. Makhoulf Brahmī, É. Derat, L. Fensterbank, E. Lacôte, M. Malacria, D. P. Curran, *J. Am. Chem. Soc.* **2008**, *130*, 10082-10083; (f) S.-H. Ueng, A. Solovyev, X. Yuan, S. J. Geib, L. Fensterbank, E. Lacôte, M. Malacria, M. Newcomb, J. C. Walton, D. P. Curran, *J. Am. Chem. Soc.* **2009**, *131*, 11256-11262; (g) T. Matsumoto, F. P. Gabbaï, *Organometallics* **2009**, *28*, 4252-4253; (h) J. C. Walton, *Angew. Chem. Int. Ed.* **2009**, *48*, 1726-1728; (i) J. C. Walton, M. M. Brahmī, L. Fensterbank, E. Lacôte, M. Malacria, Q. Chu, S.-H. Ueng, A. Solovyev, D. P. Curran, *J. Am. Chem. Soc.* **2010**, *132*, 2350-2358; (j) D. P. Curran, A. Solovyev, M. Makhoulf Brahmī, L. Fensterbank, M. Malacria, E. Lacôte, *Angew. Chem. Int. Ed.* **2011**, *50*, 10294-10317; (k) G. Wang, H. Zhang, J. Zhao, W. Li, J. Cao, C. Zhu, S. Li, *Angew. Chem. Int. Ed.* **2016**, *55*, 5985-5989; (l) A. B. Cuenca, R. Shishido, H. Ito, E. Fernández, *Chem. Soc. Rev.* **2017**, *46*, 415-430; (m) Y. Su, R. Kinjo, *Coord. Chem. Rev.* **2017**, *352*, 346-378; (n) X. Guo, Z. Lin, *Chem. Sci.* **2024**, *15*, 3060-3070.
- [2] For selected examples, see: (a) J. Lalevée, N. Blanchard, A.-C. Chany, M.-A. Tehfe, X. Allonas, J.-P. Fouassier, *J. Phys. Org. Chem.* **2009**, *22*, 986-993; (b) J. Lalevée, N. Blanchard, M.-A. Tehfe, A.-C. Chany, J.-P. Fouassier, *Chem. Eur. J.* **2010**, *16*, 12920-12927; (c) G. Wang, H. Zhang, J. Zhao, W. Li, J. Cao, C. Zhu, S. Li, *Angew. Chem. Int. Ed.* **2016**, *55*, 5985-5989; (d) F. Barth, F. Achraimer, A. M. Pütz, H. Zipse, *Chem. Eur. J.* **2017**, *23*, 13455-13464; (e) G. Wang, J. Cao, L. Gao, W. Chen, W. Huang, X. Cheng, S. Li, *J. Am. Chem. Soc.* **2017**, *139*, 3904-3910; (f) L. Zhang, L. Jiao, *J. Am. Chem. Soc.* **2017**, *139*, 607-610; (g) L. Zhang, L. Jiao, *J. Am. Chem. Soc.* **2017**, *139*, 607-610; (h) L. Zhang, L. Jiao, *Chem. Sci.* **2018**, *9*, 2711-2722; (i) L. Zhang, L. Jiao, *Chem. Sci.* **2018**, *9*, 2711-2722; (j) L. Zhang, L. Jiao, *J. Am. Chem. Soc.* **2019**, *141*, 9124-9128; (k) J. Cao, G. Wang, L. Gao, H. Chen, X. Liu, X. Cheng, S. Li, *Chem. Sci.* **2019**, *10*, 2767-2772; (l) J. Jin, H. Xia, F.-L. Zhang, Y.-F. Wang, *Chin. J. Org. Chem.* **2020**, *40*, 2185-2194; (m) T. Taniguchi, *Chem. Soc. Rev.* **2021**, *50*, 8995-9021; (n) J. H. Kim, T. Constantin, M. Simonetti, J. Lloveria, N. S. Sheikh, D. Leonori, *Nature* **2021**, *595*, 677-683; (o) L. Capaldo, T. Noël, D. Ravelli, *Chem Catal.* **2022**, *2*, 957-966; (p) Z. Ding, Z. Liu, Z. Wang, T. Yu, M. Xu, J. Wen, K. Yang, H. Zhang, L. Xu, P. Li, *J. Am. Chem. Soc.* **2022**, *144*, 8870-8882; (q) M. Xu, Z. Wang, Z. Sun, Y. Ouyang, Z. Ding, T. Yu, L. Xu, P. Li, *Angew. Chem. Int. Ed.* **2022**, *61*, e202214507; (r) T. Yu, J. Yang, Z. Wang, Z. Ding, M. Xu, J. Wen, L. Xu, P. Li, *J. Am. Chem. Soc.* **2023**, *145*, 4304-4310; (s) T. Y. Peng, F. L. Zhang, Y. F. Wang, *Acc. Chem. Res.* **2023**, *56*, 169-186; (t) F.-X. Li, X. Wang, J. Lin, X. Lou, J. Ouyang, G. Hu, Y. Quan, *Chem. Sci.* **2023**, *14*, 6341-6347; (u) Z. Wang, J. Chen, Z. Lin, Y. Quan, *Chem. Eur. J.* **2023**, *29*, e202203053; (v) J. Zeng, F. You, J. Zhu, *J. Comput. Chem.* **2024**, *45*, 648-654; (w) Y. Xie, R. Zhang, Z.-L. Chen, M. Rong, H. He, S. Ni, X.-K. He, W.-J. Xiao, J. Xuan, *Adv. Sci.* **2024**, *11*, 2306728.
- [3] For selected examples, see: (a) D. Hai-Shan, B. P. Roberts, *Tetrahedron Lett.* **1992**, *33*, 4621-4624; (b) H.-S. Dang, B. P. Roberts, *J. Chem. Soc., Perkin Trans. 1* **1993**, 891-898; (c) Y. Cai, H.-S. Dang, B. P. Roberts, *Tetrahedron Lett.* **2004**, *45*, 4405-4409; (d) S.-H.

- Ueng, L. Fensterbank, E. Lacôte, M. Malacria, D. P. Curran, *Org. Biomol. Chem.* **2011**, *9*, 3415-3420; (e) F. Juliá, T. Constantin, D. Leonori, *Chem. Rev.* **2022**, *122*, 2292-2352; (f) T. Ye, F.-L. Zhang, H.-M. Xia, X. Zhou, Z.-X. Yu, Y.-F. Wang, *Nat. Commun.* **2022**, *13*, 426; (g) X. Wu, B. Gao, *Org. Lett.* **2023**, *25*, 8722-8726.
- [4] (a) G. Lei, M. Xu, R. Chang, I. Funes-Ardoiz, J. Ye, *J. Am. Chem. Soc.* **2021**, *143*, 11251-11261; (b) Q. Shi, M. Xu, R. Chang, D. Ramanathan, B. Peñin, I. Funes-Ardoiz, J. Ye, *Nat. Commun.* **2022**, *13*, 4453.
- [5] (a) Z. Q. Zhang, Y. Q. Sang, C. Q. Wang, P. Dai, X. S. Xue, J. L. Piper, Z. H. Peng, J. A. Ma, F. G. Zhang, J. Wu, *J. Am. Chem. Soc.* **2022**, *144*, 14288-14296; (b) Z. Q. Zhang, C. Q. Wang, L. J. Li, J. L. Piper, Z. H. Peng, J. A. Ma, F. G. Zhang, J. Wu, *Chem. Sci.* **2023**, *14*, 11546-11553.
- [6] T. Wan, L. Capaldo, D. Ravelli, W. Vitullo, F. J. de Zwart, B. de Bruin, T. Noel, *J. Am. Chem. Soc.* **2022**, *145*, 991-999.
- [7] For selected examples, see: (a) H. Amii, K. Uneyama, *Chem. Rev.* **2009**, *109*, 2119-2183; (b) F. Jaroschik, *Chem. Eur. J.* **2018**, *24*, 14572-14582; (c) H.-J. Ai, X. Ma, Q. Song, X.-F. Wu, *Sci. China Chem.* **2021**, *64*, 1630-1659.
- [8] For selected reviews, see: (a) D. O'Hagan, *Chem. Soc. Rev.* **2008**, *37*, 308-319; (b) A. M. Träff, M. Janjetovic, L. Ta, G. Hilmersson, *Angew. Chem. Int. Ed.* **2013**, *52*, 12073-12076; (c) O. Eisenstein, J. Milani, R. N. Perutz, *Chem. Rev.* **2017**, *117*, 8710-8753; (d) R. Gupta, D. Csókás, K. Lye, R. D. Young, *Chem. Sci.* **2023**, *14*, 1291-1300.
- [9] For selected examples, see: (a) Y.-J. Yu, F.-L. Zhang, T.-Y. Peng, C.-L. Wang, J. Cheng, C. Chen, K. N. Houk, Y.-F. Wang, *Science* **2021**, *371*, 1232-1240; (b) T. Y. Peng, Z. Y. Xu, F. L. Zhang, B. Li, W. P. Xu, Y. Fu, Y. F. Wang, *Angew. Chem. Int. Ed.* **2022**, *61*, e202201329; (c) T.-Y. Peng, Z.-Y. Xu, F.-L. Zhang, B. Li, W.-P. Xu, Y. Fu, Y.-F. Wang, *Angew. Chem. Int. Ed.* **2022**, *61*, e202201329; (d) F.-L. Zhang, B. Li, K. N. Houk, Y.-F. Wang, *JACS Au* **2022**, *2*, 1032-1042.
- [10] P. R. Rablen, *J. Am. Chem. Soc.* **1997**, *119*, 8350-8360.
- [11] D. Lu, C. Wu, P. Li, *Chem. Eur. J.* **2014**, *20*, 1630-1637.
- [12] L. Zhang, Z. Cao, *Phys. Chem. Chem. Phys.* **2023**, *25*, 12072-12080.
- [13] S. Liu, Y.-L. Su, T.-Y. Sun, M. P. Doyle, Y.-D. Wu, X. Zhang, *J. Am. Chem. Soc.* **2021**, *143*, 13195-13204.
- [14] (a) M. G. Evans, M. Polanyi, *Trans. Faraday Soc.* **1938**, *34*, 11-24; (b) R. P. Bell, C. N. Hinshelwood, *Proc. R. Soc. Lond. A* **1997**, *154*, 414-429.
- [15] T. Constantin, B. Górski, M. J. Tilby, S. Chelli, F. Juliá, J. Llaveria, K. J. Gillen, H. Zipse, S. Lakhdar, D. Leonori, *Science* **2022**, *377*, 1323-1328.
- [16] (a) G. Knizia, *J. Chem. Theory Comput.* **2013**, *9*, 4834-4843; (b) G. Knizia, J. E. M. N. Klein, *Angew. Chem. Int. Ed.* **2015**, *54*, 5518-5522.
- [17] J. E. M. N. Klein, G. Knizia, *Angew. Chem. Int. Ed.* **2018**, *57*, 11913-11917.
- [18] (a) K. Yamamoto, J. Li, J. A. O. Garber, J. D. Rolfes, G. B. Boursalian, J. C. Borghs, C. Genicot, J. Jacq, M. van Gastel, F. Neese, T. Ritter, *Nature* **2018**, *554*, 511-514; (b) L. Zhang, J. Yan, D. Ahmadli, Z. Wang, T. Ritter, *J. Am. Chem. Soc.* **2023**, *145*, 20182-20188.
- [19] (a) J.-X. Zhang, F. K. Sheong, Z. Lin, *Chem. Eur. J.* **2018**, *24*, 9639-9650; (b) F. K. Sheong, J.-X. Zhang, Z. Lin, *Phys. Chem. Chem. Phys.* **2020**, *22*, 10076-10086; (c) J.-X. Zhang, F. K. Sheong, Z. Lin, *WIREs Comput. Mol. Sci.* **2020**, *10*, e1469.
- [20] F. Vermersch, S. Yazdani, G. P. Junor, D. B. Grotjahn, R. Jazzar, G. Bertrand, *Angew. Chem. Int. Ed.* **2021**, *60*, 27253-27257.
- [21] S. Klein, R. Tonner, G. Frenking, *Chem. Eur. J.* **2010**, *16*, 10160-10170.
- [22] D. Subervie, B. Graff, S. Nerkar, D. P. Curran, J. Lalevée, E. Lacôte, *Angew. Chem. Int. Ed.* **2018**, *57*, 10251-10256.
- [23] D. J. Sheldon, M. R. Crimmin, *Chem. Soc. Rev.* **2022**, *51*, 4977-4995.